FORMATION AND EMPLACEMENT OF THE COGENETIC NAKHLITE AND CHASSIGNITE METEORITES. A. Udry[1] and J. M. D. Day[2], [1]Department of Geoscience, University of Nevada Las Vegas, Las Vegas NV, USA, arya.udry@unlv.edu [2]Scripps Institution of Oceanography, University of California San Diego, La Jolla, CA 92093-0244, USA, jmdday@ucsd.edu.

Introduction: Nakhlites and chassignites are cumulate clinopyroxene-rich and olivine-rich martian meteorites, respectively, and include a total of 22 individual meteorites. Although they have different mineralogy, they show similar trace element compositions, volatile-bearing mineral compositions, crystallization (1340 ±40 Ma) and ejection (~11 Ma) ages, and Rb-Sr and Sm-Nd isotopic compositions [e.g, 1-7]. These similarities suggest that nakhlites and chassignites crystallize at the same time and originate from the same location on the martian surface. Various models have been proposed for their emplacement [1,2, 8-16], However, only [2] conducted a study considering both chassignites and nakhlites.

Using a comprehensive suite of nakhlites and chassignites, including 17 samples, and utilizing systematic analyses of bulk and mineral major and trace element compositions, and quantitative textural data, we constrain the link, petrogenesis, and emplacement of these rocks in the martian crust. This study includes three recent finds Northwest Africa (NWA) 11013, NWA 10645, and NWA 10153, which have not been previously investigated.

Samples and Methods: Quantitative textural analysis was conducted on pyroxene for nakhlites, and olivine for NWA 998 and both chassignites, for a total of 15 samples (see caption Fig. 1). Detailed methods of quantitative textural analyses can be found in [15]. We conducted bulk-rock analyses on the same samples as those for textural analyses, as well as for NWA 10153 and NWA 6148. Major and minor mineral element compositions were obtained using the *JEOL JXA-8900* electron microprobe analyzer housed at the University of Nevada, Las Vegas (UNLV). *In situ* trace element compositions were obtained using a *New Wave Research* UP213 (213 nm) laser-ablation (LA) system coupled with a *ThermoScientific* iCAPq Inductively Couple Plasma Mass Spectrometer (ICP-MS) at the *Scripps Isotope Geochemistry Laboratory* (SIGL). Bulk-rock major and trace element abundances were determined using solution ICP-MS techniques at SIGL [17].

Results and Discussion:

Field relationship of nakhlites and chassignites. Using quantitative textural analyses, we reviewed previous nakhlite emplacement models, inferred from various characteristics, such as modal abundances of intercumulus and cumulus phases, crystallinity of plagioclase, pyroxene rim sizes, and mineral equilibration and compositions [1,2, 8-16]. These models generally assume a single nakhlite cumulate pile.

Crystal Size Distribution (CSD) patterns indicate a negative correlation between intercept and slope for the nakhlite pyroxene population (Fig. 1), excluding NWA 10645 (longest pyroxenes) and NWA 5790 [from 15].

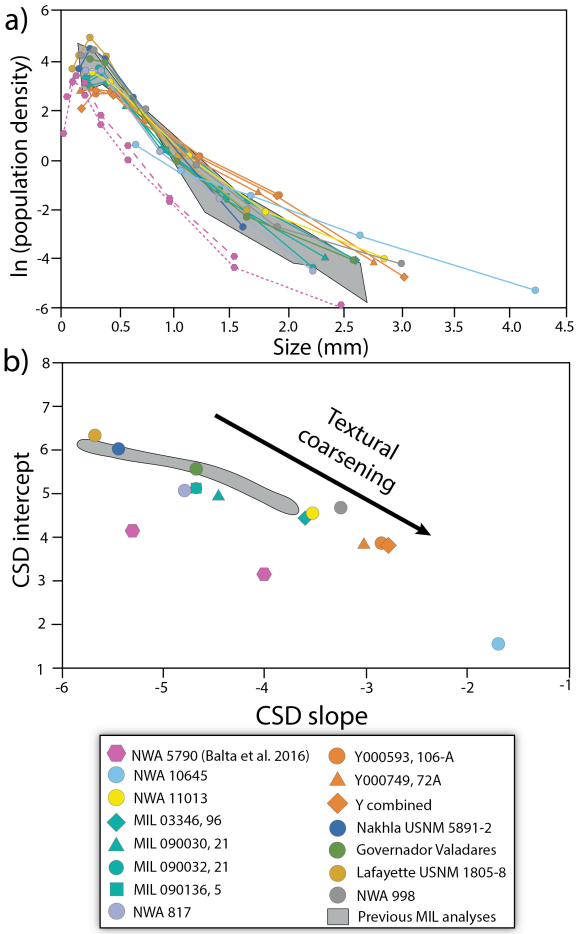

Figure 1: *CSD profiles for a) augite grains in nakhlites,: a) CSD slope versus intercepts. NWA 5790 profiles are from [15] and MIL nakhlite data are from [10] and [13].*

This trend indicates textural coarsening of the pyroxene population. Nakhla, Governador Valadares, and Lafayette show shorter residence times and higher slope:intercept ratios than the other nakhlites, whereas Yamatos display the coarsest pyroxene and longest residence time of all nakhlites. These results were not

expected based on previous cooling rate estimates of these rocks, if a single cumulate pile model is assumed. The pyroxene textures as well as presence of plagioclase in the newly found NWA nakhlites (including NWA 11013 and NWA 10645) show that they could not have been emplaced in the same cumulate pile as the other nakhlites. According to textural analyses, we suggest that nakhlites were emplaced in different lava flows or sills. In addition, the chassignite adcumulus texture and olivine homogenization suggest that they were emplaced as a thick flow or at the bottom of a sill, thus they were emplaced within a different lava flow to that of the nakhlites.

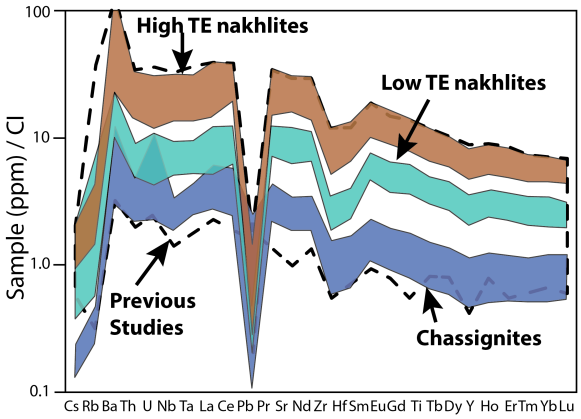

Figure 2: *CI-chondrite normalized multi-incompatible trace element for bulk-rock of nakhlites (High TE and low TE groups) and chassignites. Previous studies from [1,10-13, 18-20]*

Are nakhlites and chassignites cogenetic? Nakhlites and chassignites show coherent major element trend versus Mg# (= molar MgO/(MgO/FeO)), with increasing incompatible element with decreasing Mg#, corresponding to mesostasis modal abundance [cf. 1]. In addition, all nakhlites and chassignites display similar relative trace element and rare earth element (REE) patterns with variable absolute concentrations (Fig. 2). We can divide nakhlite into two groups: (1) high absolute trace-element abundance (high TE) nakhlites: NWA 6148, NWA 11013, NWA 10153, NWA 817, and the four Miller Range nakhlites, and (2) low absolute trace-element abundance (low TE) nakhlites, including the Yamato nakhlites, Nakhla, Governador Valadares, Lafayette, and NWA 998 (Fig. 2). Similar major and trace element compositions as well as previous isotopic analyses [e.g., 1,3] indicate that nakhlites and chassignites originate from the same source

Fractional crystallization and source melting. We can calculate the amount of fractional crystallization required to produce nakhlite bulk-rock compositions from olivine and pyroxene accumulation to form chassignites by using the relationship between MgO and other major and minor elements of nakhlites and chassignites. Assuming fractionation of the most primitive olivine (Fo_{79}) and clinopyroxene (Mg#) compositions measured in this study, we find that low TE nakhlites can be formed from removal of 10-12% olivine and 2-5% clinopyroxene from a parental melt with 15 wt. % MgO (calculated from intercept of regression MgO-FeO and MgO-Al_2O_3 between nakhlites and chassignites) indicating that formation of nakhlites involves multi-phase fractional crystallization. In addition, using trace elements, we calculate that nakhlites and chassignites formed from 1-5% partial melting with contribution from 10-20% garnet-bearing source using partial melting models for terrestrial basalts [21].

Open-system crystallization of nakhlites and chassignites. Using the most primitive pyroxene and olivine core compositions in nakhlites and chassignites (highest Mg#), respectively, and partition coefficients from [22], we calculate the parental melt REE composition of these rocks. These compositions are not consistent with the bulk-rock REE compositions, suggesting an open-system crystallization, such as fluid interaction. This was also inferred by [2], who suggested that a Cl-rich and LREE-rich exogenous fluid infiltrated the nakhlite-chassignite magma. In addition, we measured non concordant ^{207}Pb-^{206}Pb ages in an NWA 998 apatite of 3126 ±68 Ma to 4403 ±108 Ma, which is older than their crystallization ages (1.3 Ga). This suggests an inherited Pb component, likely indicating open-system process, such as addition of crustal fluid.

Acknowledgements: We thank the Smithsonian Institution, the Japanese Antarctica collection, the JSC MWG, and L. Labenne, M. Ouzillou, and G. Hupe for providing the samples.

References: [1] Treiman A. H. (2005) *Chemie Der Erde-Geochemistry* , 203–270. [2] McCubbin F. M. et al. (2013) *Meteoritics & Planet. Sci. 48*, 819-853. [3] Nyquist (2001) *JGR 90,* 1151–1154. [4] Korochantseva E. V. et al. (2011) *Meteoritics & Planet. Sci. 46*,1397–1417. [5] Herzog G. F. et al. (2014) *35 Seasons of US Antarctic Meteorites (1976-2010),* 68:153. [6] Wieler, R. et al. (2016) *Meteoritics & Planet. Sci. 51*,407-428. [7] Cohen et al. (2017) *Nature Comms 8*, 640. [8] Sautter V. et al. (2002) *EPSL* 195:223–238. [9] Beck, P. et al. (2006) *GCA 70*,2127-2139. [10] Day J. M. D. et al. (2006) *Meteoritics & Planet. Sci. 41,* 581-606. [11] Imae N. and Ikeda Y. (2007) *Meteoritics & Planet. Sci. 42*:171–184. [12] Treiman A. H. and Irving A. J. (2008) *Meteoritics & Planet. Sci. 43*, 829–854. [13] Udry A. et al. (2012) *Meteoritics & Planet. Sci. 47*, 1575-1589. [14] Corrigan C.M. (2015) *Meteoritics & Planet. Sci. 50*, 1497-1511. [15] Balta J. B. et al. (2016) *Meteoritics & Planet. Sci. 1-24.* [16] Richter F. et al. (2016) *GCA 182*, 1-23. [17] Day, J. M. D. et al. (2017) *GCA 198*, 379-395. [18] Lodders K. (1998) *Meteoritics & Planet. Sci*, *33*. [19] Jambon A. et al. (2016) *GCA* 190:191-212. [20] Yang, S et al. (2015) *Meteoritics & Planet. Sci 50*:691-714. [21] Day, J. M. D. et al. (2010) *GCA* 74:6565-6589. [22] Oe K. et al. (2001) LPS XXXII, Abstract #2174.